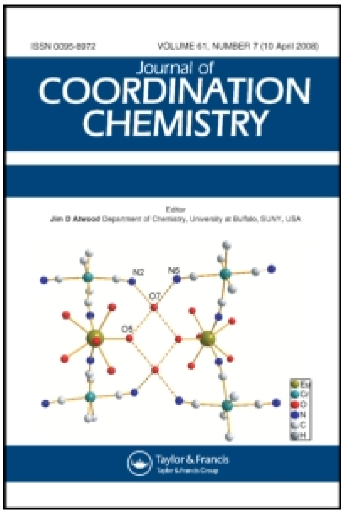

Journal of Coordination Chemistry
Publication details, including instructions for authors and subscription information:
http://www.informaworld.com/smpp/title~content=t713455674

Constructing porous lanthanide coordination polymers of 4,4'-bipyridine-<i>N</i>,<i>N</i>'-dioxide templated by single- and double-Keggin anions

Meilin Wei[a]; Ruiping Sun[a]; Kai Jiang[a]; Lin Yang[a]
[a] College of Chemistry and Environmental Science, Henan Normal University, Xinxiang, 453007, P.R. China

To cite this Article Wei, Meilin , Sun, Ruiping , Jiang, Kai and Yang, Lin(2008) 'Constructing porous lanthanide coordination polymers of 4,4'-bipyridine-<i>N</i>,<i>N</i>'-dioxide templated by single- and double-Keggin anions', Journal of Coordination Chemistry, 61: 23, 3800 — 3814

To link to this Article: DOI: 10.1080/00958970802123469

URL: http://dx.doi.org/10.1080/00958970802123469

Journal of Coordination Chemistry
Vol. 61, No. 23, 10 December 2008, 3800–3814

Taylor & Francis
Taylor & Francis Group

Constructing porous lanthanide coordination polymers of 4,4′-bipyridine-*N*,*N*′-dioxide templated by single- and double-Keggin anions

MEILIN WEI*, RUIPING SUN, KAI JIANG and LIN YANG

College of Chemistry and Environmental Science, Henan Normal University,
Xinxiang, 453007, P.R. China

(*Received 30 November 2007; in final form 18 February 2008*)

Three porous coordination polymers, $\{[Nd(dpdo)_2(H_2O)_5(CH_3OH)_2](PMo_{12}O_{40})(CH_3OH)(H_2O)_5\}_n$ (**1**), $\{[Tb(dpdo)_4(H_2O)_3](PMo_{12}O_{40})(H_2O)_2CH_3CN\}_n$ (**2**) and $\{[Tb(dpdo)_4(H_2O)_3]H(SiMo_{12}O_{40})(dpdo)_{0.5}(CH_3CN)_{0.5}(H_2O)_4\}_n$ (**3**) (where dpdo is 4,4′-bipyridine-*N*,*N*′-dioxide), templated by single- or double-Keggin polyanions were synthesized and characterized by single crystal X-ray diffraction. The compounds exhibit three different 3D non-interwoven frameworks with large cavities occupied by the single- or double-Keggin-type anions. Thermogravimetric analyses suggest different stability for the three metal-organic frameworks. The SHG (second harmonic generation) efficiency of **1** confirms its noncentric framework.

Keywords: Coordination polymer; Polyoxometalate; 4,4′-Bipyridine-*N*,*N*′-dioxide; Lanthanide complex

1. Introduction

A wide range of topologies and connectivities in the solid state has been provided by molecular and materials science. Recent studies on inorganic/organic hybrid materials, especially in the area of metal-ligand coordination polymers, have enriched this area substantially [1, 2]. 4,4′-bipyridine-*N*,*N*′-dioxide plays an important role in both lanthanide and transition metal coordination polymers resulting in extended assemblies with different topologies and different connection modes of the ligand [3]. Polyoxometalates (POMs) are an outstanding class of inorganic templates for construction of cationic coordination polymer hosts [4–13]. To access novel topologies and better understand the correlation of geometry and charge of POMs as well as organic solvents to the resultant structures, herein, Ln^{3+} ions, 4,4′-bipyridine-*N*,*N*′-dioxide [3] and different charged Keggin-type $[PMo_{12}O_{40}]^{3-}$ and $[SiMo_{12}O_{40}]^{4-}$ polyanions, as well as acetonitrile and methanol were chosen to construct POMs-templated 3D open frameworks with novel topologies and channels. The presence of nanosized, highly-charged anions as building blocks prevented occurrence of lattice interpenetration. Based on coordination, hydrogen bonding

---

*Corresponding author. Email: weimeilin@henannu.edu.cn

Journal of Coordination Chemistry
ISSN 0095-8972 print/ISSN 1029-0389 online © 2008 Taylor & Francis
DOI: 10.1080/00958970802123469

and π–π stacking interactions, three compounds with different metal-organic frameworks with large cavities occupied by the single- or double-Keggin-type anions are formed.

2. Experimental

2.1. *Materials and measurements*

All solvents and materials used for syntheses were of reagent grade and used without further purification. The metal chlorides $LnCl_3 \cdot 6H_2O$ (Ln = Tb and Nd) were prepared by dissolving Ln_2O_3 (99.9%) in hydrochloric acid followed by drying and crystallization. α-$H_3PMo_{12}O_{40} \cdot 6H_2O$ and α-$H_4SiMo_{12}O_{40} \cdot 14H_2O$ were prepared according to the literature method [14] and characterized by IR spectra and TG analyses. Elemental analyses (C, H, and N) were carried out on a Perkin-Elmer 240C analyzer. IR spectra were recorded on a VECTOR 22 Bruker spectrophotometer with KBr pellets in the 400–4000 cm^{-1} region. Thermogravimetric analyses were carried out on a Perkin-Elmer thermal analyzer in an atmosphere of N_2 with a heating rate of 10°C min^{-1} between ambient temperature and 700°C. Powder X-ray diffraction pattern was recorded on a Bruker D8 Advanced diffractometer in Bragg-Brentano geometry with Ni-filtered Cu-Kα ($\lambda = 1.542$ Å) radiation at room temperature. A pulsed Q-switched Nd:YAG laser at a wavelength of 1064 nm was used to generate an SHG signal from the sample. The backward scattered SHG light was collected using a spherical concave mirror and passed through a filter which transmits only 532 nm radiation.

2.2. *Synthesis of [Nd(dpdo)$_2$(H$_2$O)$_5$(CH$_3$OH)$_2$](PMo$_{12}$O$_{40}$)(CH$_3$OH)(H$_2$O)$_3$]$_n$ (1)*

The formation of heteropolyacid neodymium salt was accomplished by neutralization of the acid. α-$H_3PMo_{12}O_{40} \cdot 6H_2O$ (33 mg, 0.015 mmol) and $NdCl_3 \cdot 6H_2O$ (6 mg, 0.015 mmol) were dissolved in water (2 mL) and the solution was heated to saturation at 80°C in a water bath. Yellow crystals formed after cooling the saturated solution and slow evaporating at room temperature, and characterized by an IR spectrum. A buffer layer of a solution (10 mL) of methanol/water (1 : 1, v/v) was carefully layered over a 4 mL aqueous solution of 4,4′-bipyridine-*N*,*N*′-dioxide hydrate (0.05 mmol, 11 mg). Then a methanol solution (4 mL) of resultant heteropolyacid neodymium salt was carefully layered over the buffer layer. Yellow crystals appeared after 3 weeks and were collected and dried in air after quickly being washed with water. Yield: 80% based on α-$H_3PMo_{12}O_{40} \cdot 6H_2O$. Anal. Calcd for $C_{23}H_{48}N_4O_{57}NdMo_{12}P$ (%): C, 10.55; H, 1.85; N, 2.14. Found: C, 10.32; H, 1.98; N, 1.95. IR(KBr): four characteristic asymmetric vibrations resulting from heteropolyanions with the Keggin structure, ν(Mo–Oc) (798 cm^{-1}), ν(Mo–Ob) (882 cm^{-1}), ν(Mo=Ot) (960 cm^{-1}) and ν(P–Oa) (1063 cm^{-1}); four characteristic vibrations resulting from dpdo, ν(N–O) (1228 cm^{-1}), ν(ring) (1472 cm^{-1}), δ(C–H, in plane) (1180 cm^{-1}) and δ(N–O) (838 cm^{-1}), respectively.

2.3. Synthesis of $\{[Tb(dpdo)_4(H_2O)_3](PMo_{12}O_{40})(H_2O)_2CH_3CN\}_n$ (2)

Heteropolyacid terbium salt was prepared in the same way as for heteropolyacid neodymium salt from α-$H_3PMo_{12}O_{40} \cdot 6H_2O$ (41 mg, 0.02 mmol) and $TbCl_3 \cdot 6H_2O$ (8 mg, 0.02 mmol). A buffer layer of a solution (10 mL) of acetonitrile/water (3 : 2, v/v) was carefully layered over a 4 mL aqueous solution of 4,4′-bipyridine-*N*,*N*′-dioxide hydrate (0.1 mmol, 22 mg). Then an acetonitrile/water (3 : 1, v/v) solution (4 mL) of heteropolyacid terbium salt was carefully layered over the buffer layer. Orange crystals appeared after 4–5 weeks, were collected and dried in air after quickly being washed with water. Yield: 80% based on α-$H_3PMo_{12}O_{40} \cdot 6H_2O$. Anal. Calcd for $C_{42}H_{45}N_9O_{53}TbMo_{12}P$ (%): C, 17.61; H, 1.58; N, 4.40. Found: C, 17.45; H, 1.92; N, 4.57. IR(KBr): four characteristic vibrations resulting from heteropolyanions with the Keggin structure, ν(Mo–Oc) (794 cm^{-1}), ν(Mo–Ob) (880 cm^{-1}), ν(Mo=Ot) (960 cm^{-1}), ν(P–Oa) (1062 cm^{-1}); four characteristic vibrations resulting from dpdo, ν(N–O) (1233 cm^{-1}), ν(ring) (1472 cm^{-1}), δ(C–H, in plane) (1181 cm^{-1}) and δ(N–O) (838 cm^{-1}).

2.4. Synthesis of $\{[Tb(dpdo)_4(H_2O)_3]H(SiMo_{12}O_{40})(dpdo)_{0.5}(CH_3CN)_{0.5}(H_2O)_4\}_n$ (3)

Compound **3** was prepared in the same way as for **2** using α-$H_4SiMo_{12}O_{40} \cdot 14H_2O$ (40 mg, 0.02 mmol) instead of α-$H_3PMo_{12}O_{40} \cdot 6H_2O$. Orange single crystals appeared after 5 weeks and were collected and dried in air after quickly being washed with water. Yield: 82% based on α-$H_4SiMo_{12}O_{40} \cdot 14H_2O$. Anal. Calcd for $C_{46}H_{52.5}N_{9.5}O_{56}TbMo_{12}Si$ (%): C, 18.58; H, 1.78; N, 4.48. Found: C, 18.18; H, 2.12; N, 4.22. IR(KBr): four characteristic vibrations resulting from heteropolyanions with the Keggin structure, ν(Mo=Ot) (951 cm^{-1}), ν(Mo–Ob) (865 cm^{-1}), ν(Mo–Oc) (793 cm^{-1}), ν(Si–Oa) (905 cm^{-1}); four characteristic vibrations resulting from dpdo, ν(N–O) (1228 cm^{-1}), ν(ring) (1470 cm^{-1}), δ (C–H, in plane) (1181 cm^{-1}) and δ (N–O) (838 cm^{-1}).

2.5. Crystal structure and determination

Intensity data of **1**, **2** and **3** were collected on a Siemens SMART-CCD diffractometer with graphite-monochromatic Mo-Kα radiation $\lambda = 0.71073$ Å using SMART and SAINT programs [15]. The structure was solved by direct methods and refined on F^2 using full-matrix least-squares methods with SHELXTL version 5.1 [16]. For **1**, all non-hydrogen atoms except solvent water molecules and methanol molecules were refined anisotropically. For **2**, all non-hydrogen atoms except some disordered solvent molecules were refined anisotropically, and four lattice water molecules were refined disordered with the site occupancy factors (s.o.f.) being refined using free variables. For **3**, all non-hydrogen atoms except solvent water molecules and methanol molecules were refined anisotropically, and four lattice water molecules were refined disordered with the site occupancy factors (s.o.f.) being fixed at 0.5 and one acetonitrile molecule was refined disordered with the s.o.f. for the atoms in it being fixed at 0.5. Hydrogen atoms of the organic ligands were localized in their calculated positions and refined using a riding model. Hydrogen atoms of coordinated water molecules, acetonitrile molecules and methanol molecules were localized by difference Fourier maps and

Table 1. Crystal data and structure refinements for **1**, **2** and **3**.

	1	**2**	**3**
Formula	$C_{23}H_{48}N_4O_{57}NdMo_{12}P$	$C_{42}H_{45}N_9O_{53}TbMo_{12}P$	$C_{46}H_{52.5}N_{9.5}O_{56}TbMo_{12}Si$
FW	2619.14	2865.04	2972.77
Crystal system	Orthorhombic	Triclinic	Triclinic
Space group	$Cmc2_1$	$P\bar{1}$	$P\bar{1}$
Unit cells dimensions (Å, °)			
a	15.111(2)	11.795(2)	13.221(3)
b	17.344(2)	17.397(4)	16.519(4)
c	28.382(3)	18.901(4)	18.503(4)
α	90.00	92.311(3)	88.715(4)
β	90.00	97.820(3)	81.984(4)
γ	90.00	98.598(3)	83.292(4)
V (Å^3)	7438.5(15)	3792.0(14)	3974.1(15)
Z	4	2	2
D_{Calcd} (g cm^{-3})	2.339	2.509	2.484
μ (mm^{-1})	2.761	2.965	2.832
$F(000)$	4996	2736	2852
Refl. measured	18347	18980	19655
Refl. unique	6782	9387	11381
R_{int}	0.0881	0.0957	0.0328
Param. refined	489	1079	1117
Flack factor	0.49(3)		
Goodness of fitness	1.006	0.962	0.975
R_1/wR_2 $[I \geq 2\sigma(I)]$	0.0828/0.1759	0.0617/0.1570	0.0446/0.1215
$\Delta\rho_{\text{fin}}$ (max/min) (e Å^{-3})	1.551/−0.954	2.046/−3.101	1.335/−1.489

refined by fixing the isotropic temperature factors at 1.2 times that of the atom to which it was attached. Hydrogen atoms of water molecules were not treated. The crystal parameters, data collection and refinement results for the compounds are summarized in table 1. Selected bond lengths and angles are listed in tables 2–4.

3. Results and discussion

3.1. *Structure description*

Reaction of neodymium phosphomolybdates and dpdo with Nd:dpdo:$[PMo_{12}O_{40}]^{3-}$ stoichiometries of 1 : 4 : 1 in methanol/water gave **1**, which exhibited a 3D non-interwoven framework with square cavities occupied by single-Keggin-type polyanions. In **1**, each molecular unit consists of one coordinated cation $[Nd(dpdo)_2(H_2O)_5(CH_3OH)_2]^{3+}$, one polyanion $[PMo_{12}O_{40}]^{3-}$, five lattice waters and one methanol. Each Nd^{3+} ion is coordinated by nine oxygens from five aqua ligands [mean Nd–O(water) 2.507(9) Å], two coordinated methanol molecules [mean Nd–O(methanol) 2.484(5) Å] and two independent dpdo ligands [mean Nd–O(dpdo) 2.440(10) Å]; Both dpdo are terminal monodentate ligands and connect with two coordinated waters from different neighbors through hydrogen bonds. Compound **1** consists of 1D wavelike chains with double bridging linkers along the a axis with the Nd···Nd separation of 15.2 Å (figure 1). The dihedral angle between N(1) ring (the N(1)-containing pyridine ring) and N(3) ring (the N(3)-containing pyridine ring) is 1.4°, and the one between N(2) ring and N(4) ring of the terminal one is 5.2°.

Table 2. Selected bond lengths (Å) and angles (°) for **1**.

P(1)–O(1)	1.558(4)	Nd(1)–O(2W)#2	2.489(8)	O(15)–Mo(1)–O(11)	89.5(3)
P(1)–O(4)	1.553(4)	Nd(1)–O(29)#2	2.484(5)	O(22)–Mo(1)–O(11)	89.4(3)
P(1)–O(2)	1.552(4)	Nd(1)–O(1W)#2	2.503(10)	O(6)–Mo(1)–O(11)	79.2(3)
P(1)–O(3)	1.559(4)	O(2)–P(1)–O(4)	110.0(2)	O(5)–Mo(1)–O(2)	89.1(3)
Mo(1)–O(5)	1.683(8)	O(2)–P(1)–O(1)	109.5(3)	O(15)–Mo(1)–O(2)	57.9(3)
Mo(1)–O(15)	1.703(8)	O(4)–P(1)–O(1)	109.3(3)	O(6)–Mo(1)–O(2)	88.1(3)
Mo(1)–O(22)	1.826(7)	O(2)–P(1)–O(3)	109.4(3)	O(11)–Mo(1)–O(2)	69.9(2)
Mo(1)–O(6)	1.913(8)	O(4)–P(1)–O(3)	109.4(3)	O(5)–Mo(1)–O(1)	61.2(3)
Mo(1)–O(11)	2.109(8)	O(1)–P(1)–O(3)	109.2(2)	O(6)–Mo(1)–O(1)	58.6(3)
Mo(1)–O(2)	2.332(5)	O(5)–Mo(1)–O(15)	85.1(4)	O(25)–Nd(1)–O(3W)	62.0(5)
Mo(1)–O(1)#1	2.337(5)	O(25)–Nd(1)–O(2W)	70.7(3)	O(26)–Nd(1)–O(3W)	66.5(5)
Nd(1)–O(26)	2.500(12)	O(25)–Nd(1)–O(29)#2	84.76(18)	O(29)–Nd(1)–O(3W)	71.13(15)
Nd(1)–O(25)	2.379(9)	O(25)–Nd(1)–O(29)	84.76(18)	O(29)#2–Nd(1)–O(3W)	71.13(15)
Nd(1)–O(2W)	2.489(8)	O(26)–Nd(1)–O(1W)	80.1(3)	O(1W)–Nd(1)–O(1W)#2	65.2(5)
Nd(1)–O(29)	2.484(5)	O(29)–Nd(1)–O(2W)	70.6(3)	O(2W)–Nd(1)–O(2W)#2	69.8(4)
Nd(1)–O(1W)	2.503(10)	O(29)#2–Nd(1)–O(26)	78.95(18)	O(26)–Nd(1)–O(1W)#2	80.1(3)
Nd(1)–O(3W)	2.529(10)	O(29)–Nd(1)–O(26)	78.95(18)	O(2W)–Nd(1)–O(1W)	69.8(3)
		O(25)–Nd(1)–O(2W)#2	70.7(3)	O(29)–Nd(1)–O(1W)	71.4(4)

Symmetry code: #1: $-x$, y, z; #2: $-x+1$, y, z.

Table 3. Selected bond lengths (Å) and angles (°) for **2**.

P(1)–O(38)	1.521(4)	P(1)–O(37)	1.527(4)	O(38)–P(1)–O(37)	109.7(2)
P(1)–O(39)	1.525(4)	P(1)–O(40)	1.528(4)	O(37)–P(1)–O(40)	109.5(2)
Mo(1)–O(1)	1.669(5)	Tb(1)–O(41)	2.369(5)	O(38)–P(1)–O(40)	110.4(2)
Mo(1)–O(15)	1.897(4)	Tb(1)–O(45)	2.316(4)	O(39)–P(1)–O(37)	108.9(2)
Mo(1)–O(16)	1.901(4)	Tb(1)–O(1W)	2.401(5)	O(38)–P(1)–O(39)	109.3(2)
Mo(1)–O(14)	1.930(4)	Tb(1)–O(3W)	2.429(5)	O(39)–P(1)–O(40)	109.0(2)
Mo(1)–O(13)	1.934(4)	Tb(1)–O(47)	2.344(5)	O(14)–Mo(1)–O(37)	81.7(2)
Mo(1)–O(37)	2.457(4)	Tb(1)–O(48)#1	2.339(5)	O(16)–Mo(1)–O(37)	73.2(2)
Tb(1)–O(43)	2.356(5)	Tb(1)–O(2W)	2.417(4)	O(15)–Mo(1)–O(37)	84.1(2)
O(16)–Mo(1)–O(13)	87.8(2)	O(15)–Mo(1)–O(14)	84.9(2)	O(14)–Mo(1)–O(13)	86.5(2)
O(1)–Mo(1)–O(13)	101.5(2)	O(15)–Mo(1)–O(16)	90.5(2)	O(48)#1–Tb(1)–O(3W)	71.4(2)
O(45)–Tb(1)–O(43)	82.5(2)	O(47)–Tb(1)–O(41)	79.9(2)	O(41)–Tb(1)–O(1W)	72.3(2)
O(48)#1–Tb(1)–O(41)	83.7(2)	O(45)–Tb(1)–O(1W)	81.8(2)	O(47)–Tb(1)–O(1W)	76.8(2)
O(45)–Tb(1)–O(47)	76.0(2)	O(48)#1–Tb(1)–O(47)	76.3(2)	O(43)–Tb(1)–O(1W)	73.0(2)
O(41)–Tb(1)–O(2W)	72.5(2)	O(44)#1–Tb(1)–O(1W)	68.0(2)	O(2W)–Tb(1)–O(3W)	73.2(2)
O(48)#1–Tb(1)–O(2W)	75.9(2)	O(45)–Tb(1)–O(3W)	70.1(2)	O(43)–Tb(1)–O(2W)	69.2(2)

Symmetry code: #1: $-x+1$, $-y+1$, $-z+1$.

Hydrogen bonds between two symmetry related coordinated water molecules O(1W) and O(1WA) and an oxygen atom O(27B) from a neighbor parallel terminal ligand, as well as between two symmetry related coordinated water molecules O(2W) and O(2WA) and O(28A) stabilize the chain. Face-to-face π–π stacking interactions within these bridging pairs also stabilize the chain. As shown in figure 2, adjacent parallel chains are linked through hydrogen bonds between coordinated water molecules O(2W) and 1D zigzag water chains, O(4W)–O(5W)–O(6W)–O(5WA)–O(4WA) [hydrogen bond distances (Å): O(2W)$\cdots$O(4W) 2.84(3), O(4W)$\cdots$O(5W) 2.70(2), O(5W)$\cdots$O(6W) 2.39(3); symmetry code A: $-x$, y, z], to form a 2D sheet with square lattices, thus each Nd^{3+} center is a four-connected node. These sheets arrange themselves in an $\cdots$ABABAB$\cdots$ fashion (figure S1). Being heavy "building stones" for charge compensation, $[PMo_{12}O_{40}]^{3-}$ anions position at two sides of each sheet, above and below the voids of the tetragons (figure 2) and connect adjacent sheets giving a 3D

Table 4. Selected bond lengths (Å) and angles (°) for **3**.

Si(1)–O(38)	1.617(4)	Si(1)–O(37)	1.621(5)	O(38)–Si(1)–O(37)	109.3(2)
Si(1)–O(39)	1.629(4)	Si(1)–O(40)	1.626(4)	O(37)–Si(1)–O(40)	109.1(2)
Mo(1)–O(1)	1.690(5)	Tb(1)–O(2W)	2.377(5)	O(38)–Si(1)–O(40)	110.1(2)
Mo(1)–O(17)	1.885(5)	Tb(1)–O(43)	2.354(5)	O(37)–Si(1)–O(39)	108.9(2)
Mo(1)–O(16)	1.889(4)	Tb(1)–O(47) 2.375(4)	2.330(5)	O(38)–Si(1)–O(39)	109.9(2)
Mo(1)–O(13)	1.912(5)	Tb(1)–O(44)#1		O(40)–Si(1)–O(39)	109.5(2)
Mo(1)–O(15)	1.948(5)	Tb(1)–O(45)	2.349(5)	O(17)–Mo(1)–O(16)	86.7(2)
Mo(1)–O(40)	2.330(4)	Tb(1)–O(1W)	2.375(6)	O(17)–Mo(1)–O(13)	89.7(2)
Tb(1)–O(41)	2.427(5)	Tb(1)–O(3W)	2.388(5)	O(16)–Mo(1)–O(15)	88.5(2)
O(15)–Mo(1)–O(40)	74.0(2)	O(17)–Mo(1)–O(40)	85.9(2)	O(13)–Mo(1)–O(15)	87.5(2)
O(13)–Mo(1)–O(40)	73.9(2)	O(16)–Mo(1)–O(40)	84.6(2)	O(47)–Tb(1)–O(3W)	72.6(2)
O(45)–Tb(1)–O(47)	72.8(2)	O(43)–Tb(1)–O(41)	77.1(2)	O(43)–Tb(1)–O(3W)	73.8(2)
O(44)#1–Tb(1)–O(47)	71.0(2)	O(45)–Tb(1)–O(1W)	82.3(2)	O(2W)–Tb(1)–O(3W)	69.7(2)
O(45)–Tb(1)–O(43))	79.6(2	O(45)–Tb(1)–O(41)	78.0(2)	O(44)#1–Tb(1)–O(3W)	79.7(2)
O(2W)–Tb(1)–O(41)	68.7(2)	O(44)#1–Tb(1)–O(1W)	66.7(2)	O(1W)–Tb(1)–O(41)	66.3(2)
O(44)#1–Tb(1)–O(2W)	89.2(2)			O(1W)–Tb(1)–O(2W)	85.7(2)

Symmetry code: #1: $x+1$, y, z.

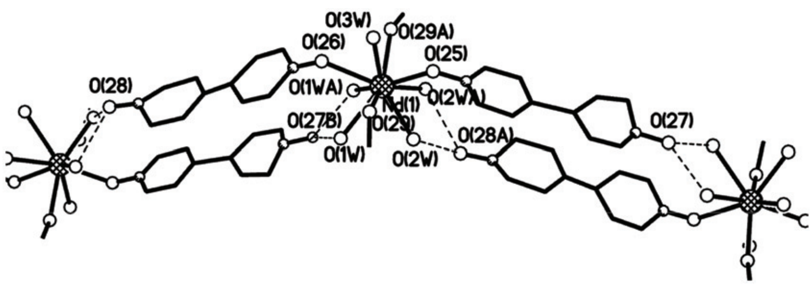

Figure 1. A 1D chain along the a axis showing the coordination environment of Nd^{3+}. Hydrogen bond distances (Å): O(1W)···O(27B) 2.57(2), O(2W)···O(28A) 2.90(2). Symmetry code: A: $-x+1$, $-y+1$, $-0.5+z$; B: $-x+1$, $-y+1$, $0.5+z$.

framework through weak hydrogen bonds between coordinated water molecules O(1W) and the terminal oxygen atoms O(21) of polyanions [O(1W)···O(21A) 3.55(2) Å, symmetry code A: x, $-y+1$, $0.5+z$] (figure S2). $[PMo_{12}O_{40}]^{3-}$ anions as pillars fill in the wavelike channels. The solvent methanol molecule and other lattice water molecules are held in the channels through weak hydrogen bonds.

Reaction of terbium phosphomolybdate and dpdo with a Tb:dpdo:$[PMo_{12}O_{40}]^{3-}$ stoichiometry of 1 : 4 : 1 in acetonitrile/water by the layering method gave **2**, which exhibited a 3D non-interwoven framework with distorted honeycomb cavities occupied by two hydrogen-bonded Keggin-type polyanions. In **2**, each molecular unit consists of one coordinated cation $[Tb(dpdo)_4(H_2O)_3]^{3+}$, one polyanion $[PMo_{12}O_{40}]^{3-}$, two crystal waters and one acetonitrile. Each Tb^{3+} ion is coordinated in a distorted square antiprismatic geometry by eight oxygens from three aqua ligands [mean Tb–O(water) 2.380(5) Å], and from four independent dpdo ligands and a symmetry related dpdo [mean Tb–O(dpdo) 2.390(5) Å]. The dihedral angle between the N(1) ring (the N(1)-containing pyridine ring) and the N(2) ring of the bridging dpdo ligand is 9.1°, the one between N(3) ring and N(4) ring of the terminal is 7.8°, between N(5) ring and N(6) ring is 21.0°, and between N(7) ring and N(8) ring is 19.2°. Of the four independent dpdo ligands, one containing O(47) and O(48) behaves as a bridging ligand to link two

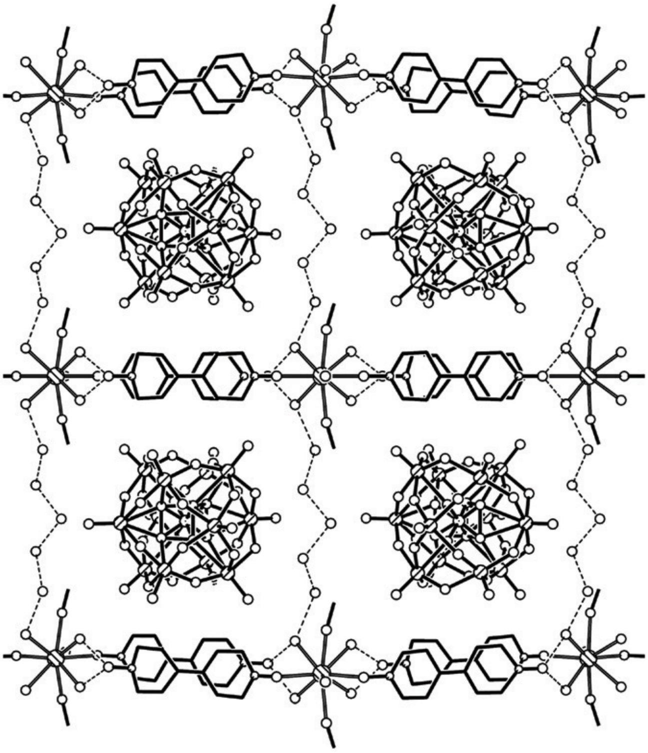

Figure 2. A 2D sheet along the *b* axis showing square lattices occupied by $[PMo_{12}O_{40}]^{3-}$.

identical metal centers in a centro-symmetrical dimer, while the other three are terminal monodentate ligands connecting with one coordinated water from different neighbors through hydrogen bonds. Each of the three coordinated waters, O(1W), O(2W) and O(3W), connects to the symmetric dpdo resulting in three centro-symmetrical doubly two-fold hydrogen bonding linkers. Thus a Tb^{3+} is a four-connected node (figure 3), and $[Tb(dpdo)_4(H_2O)_3]^{3+}$ units form a 3D non-interwoven 6^4 network with distorted honeycomb cavities along the *a* axis and voids of the tetragons along *b* (figure 4) are occupied by two centro-symmetrical Keggin ions in a shoulder by shoulder mode in each pore (figure 5). In the dimer, there are some short atom···atom separations O(8)···O(3A) 3.23(2) and O(8)···O(20A) 3.31(2) Å (symmetry code A: $-x$, $1-y$, $2-z$). The intermolecular π–π stacking interactions between the pyridine rings within each pair of centro-symmetrical double-bridging linker stabilize the framework. Partial overlap between neighboring dpdo ligands are observed in the crystal. The centroid distances of 3.811 Å between the N(1)–ring and the symmetry-related N(2)–ring ($-x$, $-y$, $1-z$), 3.811 Å between the N(2)–ring and the symmetry-related N(1)–ring ($-x, -y, 1-z$), 3.784 Å between the N(3)–ring and the symmetry-related N(4)–ring ($1-x, -y$, $2-z$), 3.784 Å between the N(4)–ring and the symmetry-related N(3)–ring ($1-x, -y$, $2-z$), 4.391 Å between the N(5)–ring and the symmetry-related N(6)–ring ($1-x, 1-y, 2-z$), 4.391 Å between the N(6)–ring and the symmetry-related N(5)–ring ($1-x, -y, -z+2$), 3.539 Å between the N(7)–ring and the symmetry-related N(8)–ring ($1-x, 1-y, 1-z$), 3.539 Å between the N(8)–ring and the symmetry-related N(7)–ring ($1-x, -y, 1-z$),

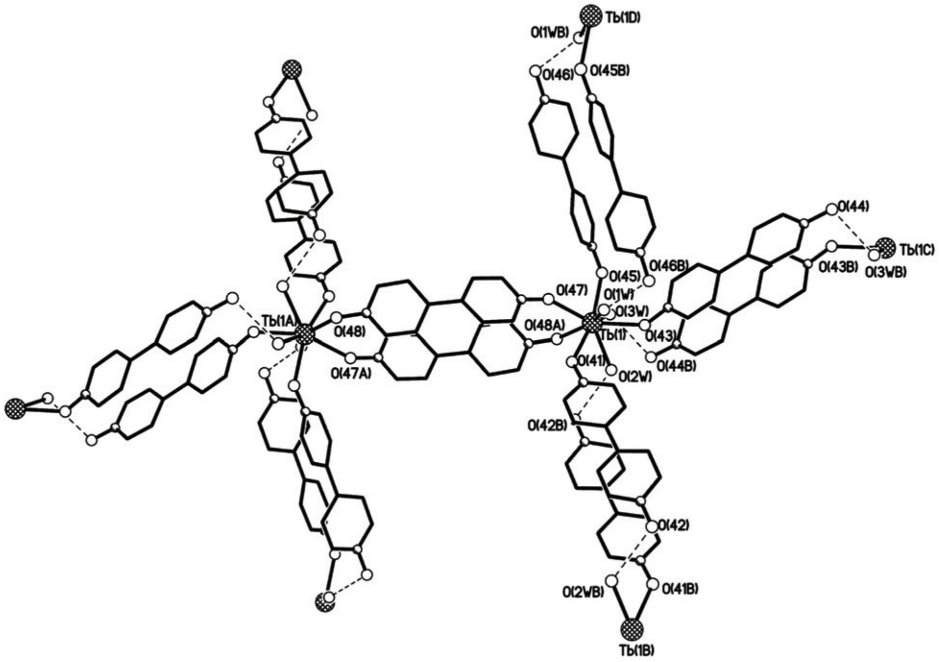

Figure 3. Perspective of the coordinated geometry of Tb^{3+} in **2** showing the four-connected node through the centro-symmetrical double bridging linkers. Hydrogen atoms of the ligands are omitted for clarity. Hydrogen bond distances (Å): O(1W) $\cdots$ N(9A) 2.84(2), O(2W) $\cdots$ O(44C) 2.83(2), O(2W) $\cdots$ O(42D) 2.79(2), O(3W) $\cdots$ O(44B) 2.85(2). Symmetry code: A: $1-x$, $1-y$, $1-z$; B: $1-x$, $1-y$, $1-z$; C: $1-x$, $-y$, $2-z$; D: $-x$, $-y$, $1-z$.

clearly suggest aromatic π–π stacking interactions. The acetonitrile and disordered lattice water molecules [O(4W), O(5W), O(6W) and O(7W)] are present in the channels.

Replacing the $[PMo_{12}O_{40}]^{3-}$ in **2** by $[SiMo_{12}O_{40}]^{4-}$ gave **3**, which exhibits a 3D non-interwoven framework with large cavities occupied by double-Keggin-type polyanions. A molecular unit consists of one coordinated cation $[Tb(dpdo)_4(H_2O)_3]^{3+}$, one polyanion $[SiMo_{12}O_{40}]^{4-}$, a half of a free dpdo, four crystal water molecule and a half of an acetonitrile molecule. The dihedral angle between N(3) ring and the N(4) ring of the bridging dpdo ligand is 24.3°, the one between the N(1) ring and the N(2) ring of the terminal one is 23.1°, another one between the N(5) ring and the N(6) ring of the terminal one is 5.8°, and the last one between the N(7) ring and the N(8) ring of the terminal one is 3.5°. The Tb^{3+} is coordinated by eight oxygens from three water molecules [mean Tb–O(water) 2.380(5) Å] and from four independent dpdo ligands and a symmetry-related dpdo ligand [mean Tb–O(dpdo) 2.390(5) Å]. As shown in figure 6, **3** consists of 1-D chain polymers along the *a* axis with Tb $\cdots$ Tb separation of 13.2 Å. Hydrogen bonds between a coordinated water O(1W) and O(42A) from a neighbor parallel terminal ligand stabilize the chains. Two adjacent 1D chains construct a one-dimensional ribbon through centro-symmetrically related two-fold hydrogen bonds formed by one of the other two terminal dpdo ligands containing O(47) and O(48B) with a coordinated water molecule O(3W) from the centro-symmetrically related lanthanide. Face-to-face π–π stacking interactions within these bridging pairs also stabilize the ribbons. Partially overlapping arrangements between neighboring

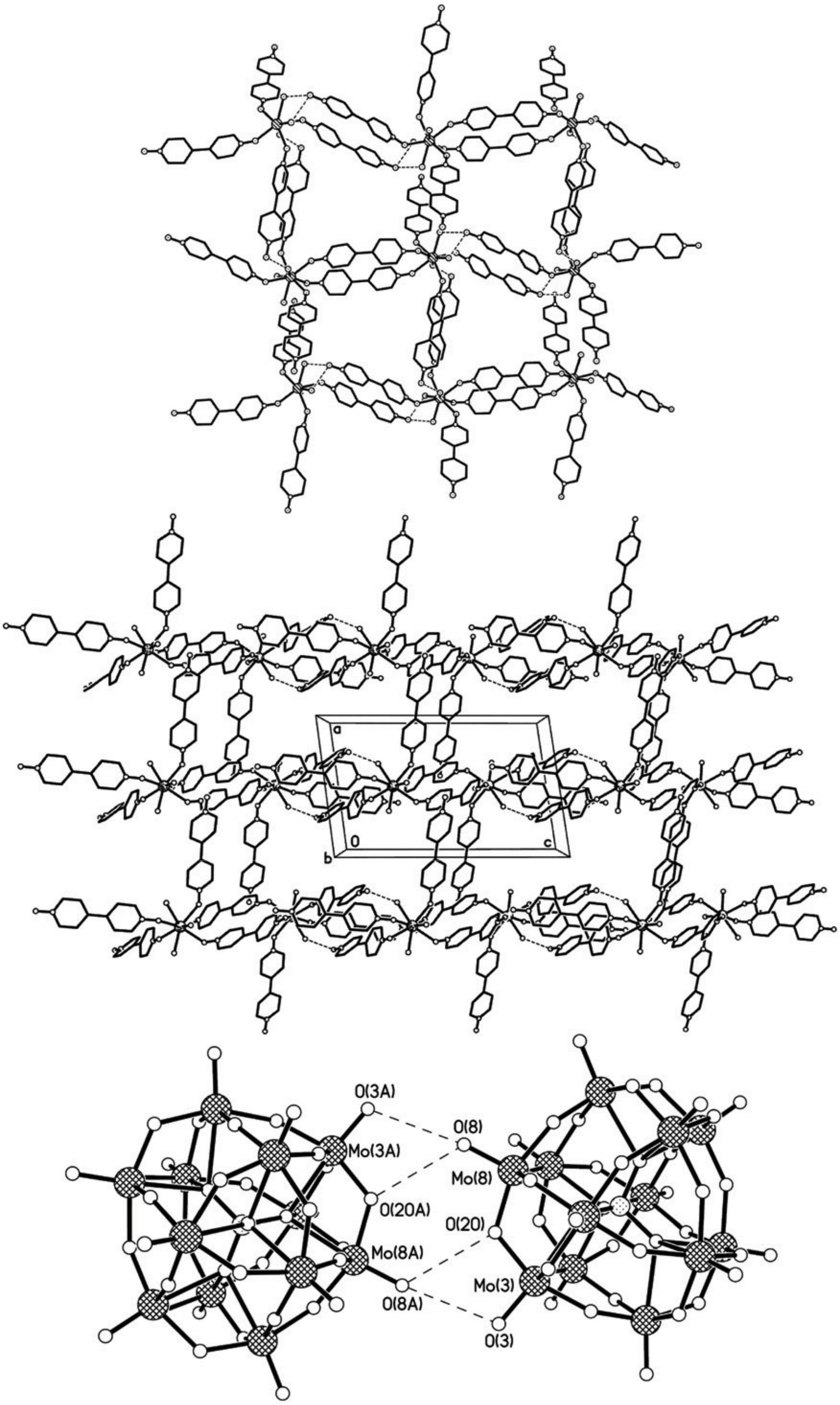

Figure 4. A 3D 6^4 network formed by $[Tb(dpdo)_4(H_2O)_3]^{3+}$ units in **2** (top), the packing diagram along the *b* axis showing the voids of the tetragons (middle), and the double-Keggin anions (bottom). Selected atom···atom separations (Å): O(8)···O(3A) 3.23(2), O(8)···O(20A) 3.31(2). Symmetry code A: $1-x$, $1-y$, $1-z$. Hydrogen atoms and the lattice solvent molecules are omitted for clarity.

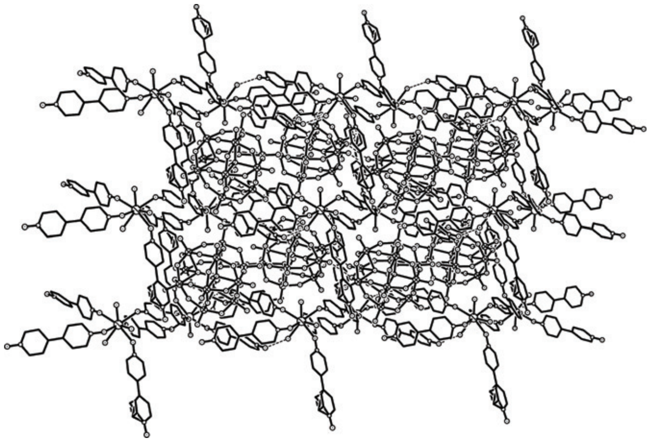

Figure 5. The voids of tetragons along the *b* axis occupied by double-Keggin polyanions in **2**. Hydrogen atoms and the lattice solvent molecules are omitted for clarity.

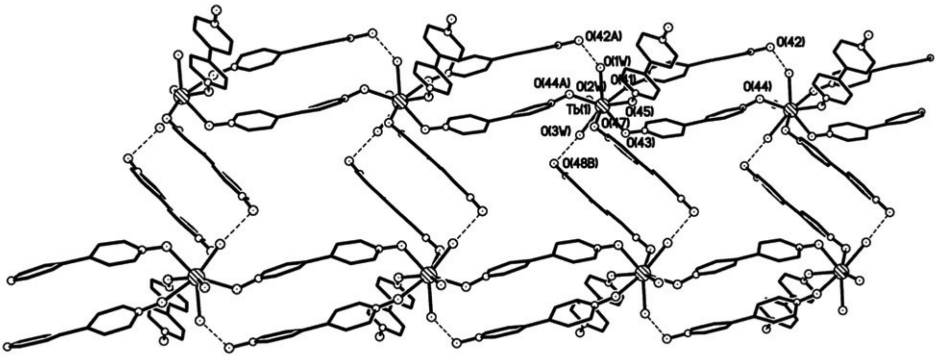

Figure 6. View of the 1D ribbon based on $[Tb(dpdo)_4(H_2O)_3]^{3+}$ units in **3**. Hydrogen atoms are omitted for clarity. Hydrogen bond distances (Å): O(1W)···O(42A) 2.59(2), O(2W)···O(4WC) 2.74(2), O(3W)···O(48B) 2.68(2), O(3W)···O(49) 2.84(2), O(4W)···O(49B) 2.76(2). Symmetry code: A: $1+x$, y, z; B: $2-x$, $1-y$, $1-z$; C: x, $1+y$, z.

dpdo ligands are observed in the crystal. The centroid distances of 3.545 Å between the N(1)–ring and the N(3)–ring, 3.738 Å between the N(2)–ring and the N(4)–ring, 3.811 Å between the N(7)–ring and the symmetry-related N(8)–ring ($-x+2$, $-y+1$, $-z+1$), and 3.811 Å between the N(8)–ring and the symmetry-related N(7)–ring ($-x+2$, $-y+1$, $-z+1$) clearly suggest π–π stacking interactions. Adjacent ribbons are linked through π–π stacking interactions between the N(5)–ring and the symmetry-related N(6)–ring ($-x+2$, $-y+1$, $-z$) (centroid distances of 3.798 Å), as well as between the N(6)–ring and the symmetry-related N(5)–ring ($-x+2, -y+1, -z$) (centroid distances of 3.798 Å) to form a 2D layer (figure 7). Adjacent layers are linked through hydrogen bonds between O(49) of the free dpdo and the coordinated water O(3W) to form a 3D network, stabilized by intermolecular π–π stacking interactions between the free and the coordinated dpdo ligands with a centroid distance of 3.936 Å between the N(3)– and N(9)–rings, as well as by hydrogen bonds among one lattice water molecule O(4W),

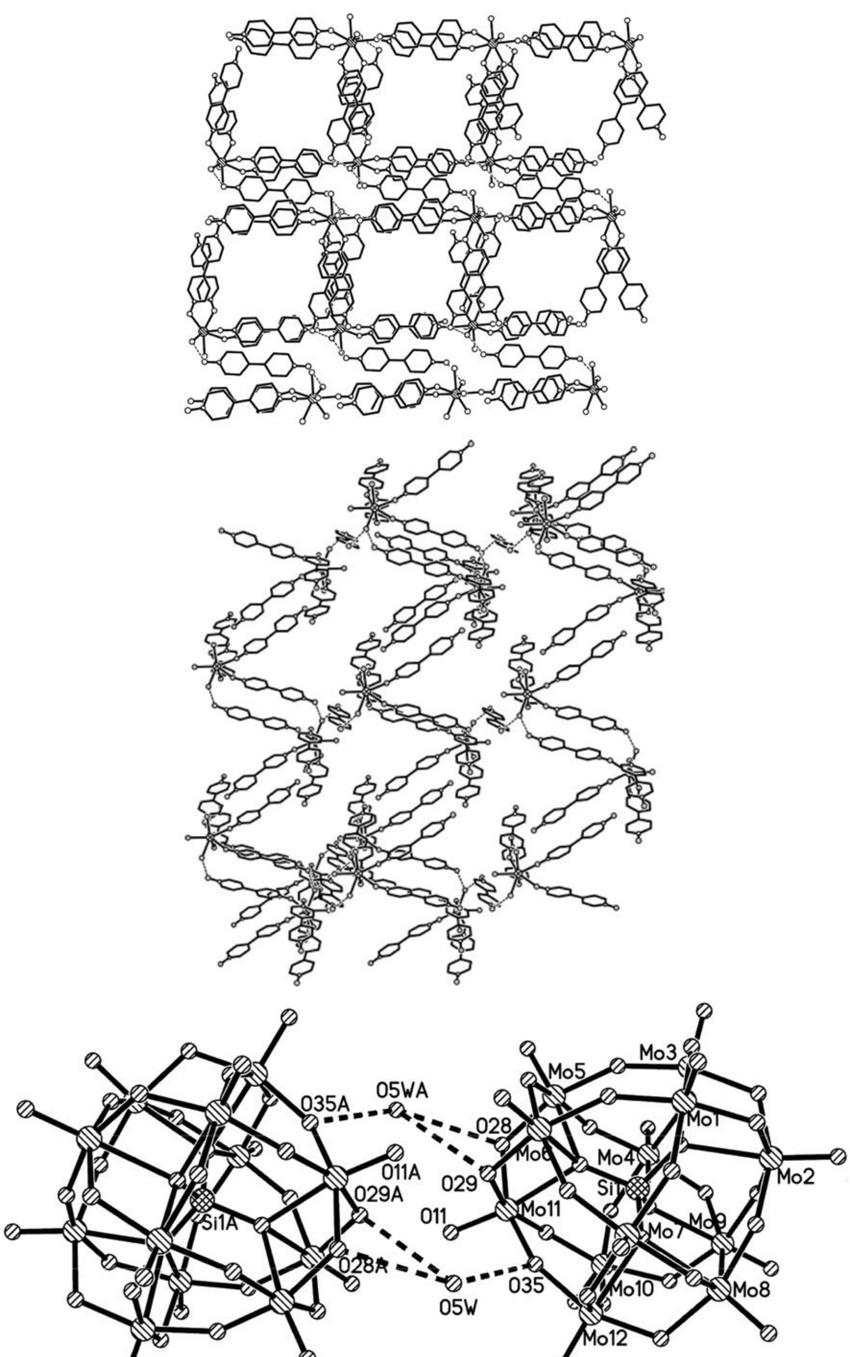

Figure 7. The 2D layer in **3** with the uncoordinated dpdo molecules as hydrogen bonding bridges (top), packing diagram of the 3D structure stabilized by the interlayer stacking interactions between dpdo ligands (middle), and the double-Keggin anions (bottom). Selected atom ⋯ atom separations (Å): O(5W) ⋯ O(28A) 3.18(2), O(5W) ⋯ O(29A) 3.15(2), O(5W) ⋯ O(35) 3.05(2), O(29) ⋯ O(11A) 3.4 Å. Symmetry code A: $1-x$, $1-y$, $1-z$. Hydrogen atoms and solvent molecules of crystallization are omitted for clarity.

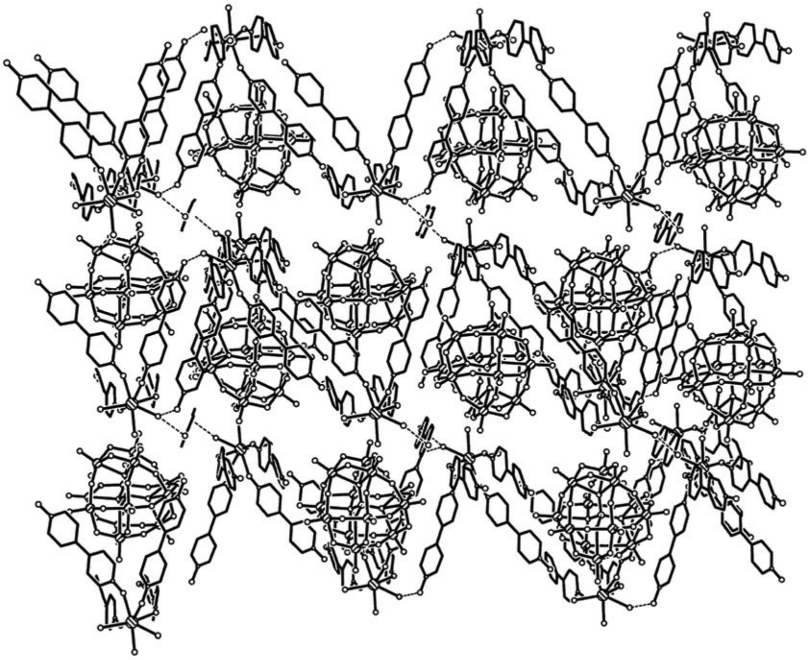

Figure 8. Packing diagram of the 3D structure of **3** with each void occupied by a shoulder-by-shoulder dimeric polyanion. Hydrogen atoms and solvent molecules are omitted for clarity.

one coordination water molecule O(2W) and the oxygen atom O(49) from a free ligand. The stacked aromatic rings divide the framework into voids (figure 7) with a centro-symmetrically related shoulder-by-shoulder dimeric anion embedded in each void (figure 8).

Though the basic structure of **3** could be determined easily based on the X-ray structure analysis, it is not clear whether its protons sit near one of the oxygens of the polyanion, near one of the oxygens of the free dpdo ligand or around the waters. It was reported that based on high-resolution solid-state ^{1}H and ^{31}P NMR that at least three different states exist for protons of $H_3PW_{12}O_{40}\cdot nH_2O$: (i) protons present in highly hydrated samples, (ii) protonated water which is hydrogen-bonded to terminal oxygen atoms, $W{=}O\cdots H^+\ (H_2O)_2$ ($n=6$), and (iii) a proton which is directly bonded to a bridging oxygen, W–OH–W ($n=0$) [17]. More recently, it was reported that based on REDOR experiments, acidic protons are localized on both bridging (Oc) and terminal (Od) oxygens of the Keggin unit in the anhydrous state of $H_3PW_{12}O_{40}$ [18]. In **3**, there are four crystal water molecules and the separations between them are too long to stabilize the excess proton, so, the excess proton is not localized on the surface of the polyanion and not able to form oligomers $H_5O_2^+$ or $H_7O_3^+$. Dpdo with N-oxide groups having formal partial negative and positive charges on the oxygen and nitrogen atoms, respectively, may be protonated at the oxygen atoms, but to our knowledge, no examples of such protonation have been reported. Since the O(5W) centers are located close to the polyanions with two shoulder-by-shoulder polyanions forming a double-Keggin anion (figure 7), the probable position of the excess proton is at the O(5W) center, with the presence of the positively charged species attracting the anions [12b].

In each of these anions, there are some short atom···atom separations: O(5W)···O(28A) 3.18(2), O(5W)···O(29A) 3.15(4), O(5W)···O(35) 3.05(2) and O(11)···O(29A) 3.34(4) Å (symmetry code A: $-x+1$, $-y+1$, $-z+1$).

In **1**, the P–O and Mo–O bond lengths are 1.552(4)–1.559(4) and 1.437(11)–2.486(5) Å, respectively. In **2**, the P–O and Mo–O bond lengths are 1.521(4)~1.528(4) and 1.667(5)~2.457(4) Å, respectively, comparable to those of 1.524(5)–1.535(5) and 1.662(6)–2.446(5) Å, respectively, in $\{Gd(dpdo)_4(H_2O)_5(PMo_{12}O_{40})(CH_3CN)\}_n$ [12b], and 1.529(6)–1.532(3) and 1.683(3)–2.435(2) Å, respectively, in $\{[Cu(2\text{-}Mepz)_{1.5}]_3(PMo_{12}O_{40})(H_2O)_{3.5}\}_n$ [11c]. In **3**, the Si–O and Mo–O bond lengths are 1.617(4)–1.629(4) and 1.665(5)–2.359(4) Å, respectively, comparable to those of 1.607(5)–1.624(5) and 1.655(6)–2.357(5) Å in $\{Gd(dpdo)_4(H_2O)_3H(SiMo_{12}O_{40})](dpdo)_{0.5}(CH_3CN)_{0.5}(H_2O)_4\}_n$ [12b]. These polyanions have normal Keggin structures. The compounds all form supramolecular networks with 3D tunnels, and the sizes of the tunnels are ca 10.4 × 10.4 Å for **1**, 10.4 × 21.4 Å for **2** and 10.4 × 21.1 Å for **3**, based on the sizes of the Keggin anions. In **1**, each pore could only house one Keggin ion, while, in **2** and **3**, each pore is large enough to accommodate two centro-symmetrical Keggin ions in a shoulder by shoulder mode. These single- and double-Keggin anions may serve as templates during the assembly so that the cationic frameworks are aggregated around them, leading to large-pore supramolecular networks [9, 12]; the non-coordinating single- and double-Keggin-type anions play not only a charge-compensating role, but influence the overall solid-state architecture through their templating. Thus, this strategy provides a new approach to novel topologies and to develop better understanding of the formation of double-Keggin anions within the resultant structures. The same Ln : dpdo : $[PMo_{12}O_{40}]^{3-}$ ($[SiMo_{12}O_{40}]^{4-}$) 1 : 4 : 1 stoichiometry and the same synthesis gave three metal-organic frameworks with different topologies based on coordination, hydrogen bonding and π–π stacking interactions, suggesting that the charge of polyanions and nature of solvent influences self-assembly of metal-organic frameworks.

3.2. *SHG measurement*

Since **1** crystallizes in a noncentrosymmetric space group, preliminary SHG response of this complex was estimated by measuring the powder of the crystalline sample of **1** (ca 80–120 µm in diameter, Kurtz powder test) relative to urea [19]. The SHG efficiency of **1** is approximately 0.3 times of that of urea, confirming its noncentric framework. The powder X-ray diffraction data and the simulated powder pattern from single-crystal data of **1** are almost consistent (figure S5), thus, the SHG reflects the molecular arrangement in the crystals.

3.3. *Thermogravimetric analyses*

Thermogravimetric analysis of **1** in N_2 (figure S8) shows a weight loss of 10.31% in the temperature range 20–335°C, corresponding to five water molecules, one methanol, five coordinated waters and two coordinated methanols (Calcd. 10.54%). The weight loss in the temperature range 335–700°C corresponds to the loss of dpdo ligands and the disruption of the structural skeletons of the $[PMo_{12}O_{40}]^{3-}$. Thermogravimetric analyses of **2** in an atmosphere of N_2 (figure S8) show weight loss of 3.02% in the temperature range 25–155°C, corresponding to two waters and one acetonitrile (Calcd 2.69%). There is no weight loss in the temperature range 155–230°C, and the framework began to slowly decompose at 230°C due to loss of three coordinated waters. Thermogravimetric analyses of **3** in N_2 (figure S8) show a weight loss of 4.66% in the temperature range 25–200°C, corresponding to four waters, three coordinated water molecules and a half of an acetonitrile (Calcd 4.93%). There is no weight loss in the temperature range 200–350°C, and the anhydrous product began to rapidly discompose at 350°C. The thermogravimetric analyses suggest that three metal-organic frameworks have different thermal stabilities.

4. Conclusions

We synthesized three porous metal coordination polymers with different architectures from dpdo ligands and Ln(III) ions (Nd^{3+} and Tb^{3+}) in methanol/water or acetonitrile/water solutions directed by single- or double-Keggin-type anions as templates. These compounds provide examples for better understanding the template effect of single- or double-Keggin-type anions and the effect of methanol and acetonitrile on the resultant structures.

Supplementary material

Crystallographic data for **1**, **2** and **3** have been deposited at the Cambridge Crystallographic Data Centre, CCDC-661938(**1**), CCDC-658011(**2**) and CCDC-658012(**3**). The data can be obtained free of charge from the Director, CCDC, 12 Union Road, Cambridge, CB2 1EZ, UK; Fax: +44-1223/336-033; E-mail: deposit@ccdc.cam.ac.uk or www.ccdc.cam.ac.uk/conts/retrieving.html

Acknowledgement

This work is supported by the Natural Science Foundation of Henan Province.

References

[1] M. Eddaoudi, D.B. Moler, H.L. Li, B.L. Chen, T.M. Reineke, M. O'Keeffe, O.M. Yaghi. *Acc. Chem. Res.*, **34**, 319 (2001).

[2] B. Moulton, M.J. Zaworotko. *Chem. Rev.*, **101**, 1629 (2001).

[3] (a) B.Q. Ma, S. Gao, H.L. Sun, G.X. Xu. *J. Chem. Soc., Dalton Trans.*, 130 (2001); (b) D. Long, A.J. Blake, N.R. Champness, M. Schröder. *Chem. Commun.*, 2273 (2000); (c) D. Long, R.J. Hill, A.J. Blake, N.R. Champness, P. Hubberstey, D.M. Proserpio, C. Wilson, M. Schröder. *Angew. Chem. Int. Ed.*, **43**, 1851 (2004).

[4] (a) S. Kitagawa, R. Kitaura, S. Noro. *Angew. Chem., Int. Ed.*, **43**, 2334 (2004); (b) J.S. Seo, D. Whang, H. Lee, S.I. Jun, J. Oh, Y.J. Jeon, K. Kim. *Nature*, **404**, 982 (2000).

[5] (a) C.D. Wu, A. Hu, L. Zhang, W. Lin. *J. Am. Chem. Soc.*, **127**, 8940 (2005); (b) L. Pan, D.H. Olson, L.R. Ciemnolonski, R. Heddy, J. Li. *Angew. Chem., Int. Ed.*, **45**, 616 (2006).

[6] D. Long, E. Burkholder, L. Cronin. *Chem. Soc. Rev.*, **36**, 105 (2007).

[7] (a) T. Ruther, V.M. Hultgren, B.P. Timko, A.M. Bond, W.R. Jackson, A.G. Wedd. *J. Am. Chem. Soc.*, **125**, 10133 (2003); (b) A. Müller, S.K. Das, S. Talismanov, S. Roy, E. Beckmann, H. Bögge, M. Schmidtmann, A. Merca, A. Berkle, L. Allouche, Y. Zhou, L. Zhang. *Angew. Chem. Int. Ed.*, **42**, 5039 (2003).

[8] (a) S. Uchida, R. Kawamoto, T. Akatsuka, S. Hikichi, N. Mizuno. *Chem. Mater.*, **17**, 1367 (2005); (b) R. Kawamoto, S. Uchida, N. Mizuno. *J. Am. Chem. Soc.*, **127**, 10560 (2005); (c) C. Jiang, A. Lesbani, R. Kawamoto, S. Uchida, N. Mizuno. *J. Am. Chem. Soc.*, **127**, 14240 (2006).

[9] (a) H.-A. An, E.-B. Wang, D.-R. Xiao, Y.-G. Li, Z.-M. Su, L. Xu. *Angew. Chem., Int. Ed.*, **45**, 904 (2006); (b) Y.-G. Li, L.-M. Dai, Y.-H. Wang, X.-L. Wang, E.-B. Wang, Z.-M. Su, L. Xu. *Chem. Commun.*, 2593 (2007); (c) J. Lu, E.-H. Shen, Y.-G. Li, D.-R. Xiao, E.-B. Wang, L. Xu. *Cryst. Growth Des.*, **5**, 65 (2005).

[10] (a) J. Kang, B. Xu, Z. Peng, X. Zhu, Y. Wei, D.R. Powell. *Angew. Chem., Int. Ed.*, **44**, 6902 (2005); (b) J.M. Knaust, C. Inman, S.W. Keller. *Chem. Commun.*, 492 (2004).

[11] (a) Y.-P. Ren, X.-J. Kong, X.-Y. Hu, M. Sun, L.-S. Long, R.-B. Huang, L.-S. Zheng. *Inorg. Chem.*, **45**, 4016 (2006); (b) P.Q. Zheng, Y.P. Ren, L.S. Long, R.B. Huang, L.S. Zheng. *Inorg. Chem.*, **44**, 1190 (2005); (c) X.-J. Kong, Y.-P. Ren, P.-Q. Zheng, Y.-X. Long, L.-S. Long, R.-B. Huang, L.-S. Zheng. *Inorg. Chem.*, **45**, 10702 (2006).

[12] (a) M.-L.Wei, C. He, W.-J. Hua, C.-Y. Duan, S.-H. Li, Q.-J. Meng. *J. Am. Chem. Soc.*, **128**, 13318 (2006); (b) M.-L. Wei, C. He, Q.-Z. Sun, Q.-J. Meng, C.-Y. Duan. *Inorg. Chem.*, **46**, 5957 (2007).

[13] (a) J.-Y. Niu, M.-L. Wei, J.-P. Wang, D.-B. Dang. *Eur. J. Inorg. Chem.*, **2004**, 160 (2004); (b) J.-P. Wang, M.-L. Wei, J.-W. Zhao, J.-Y. Niu. *J. Coord. Chem.*, **59**, 1261 (2006).

[14] R.D. Claude, F. Michel, F. Raymonde, T. Rene. *Inorg. Chem.*, **22**, 207 (1983).

[15] *SMART and SAINT, Area Detector Control and Integration Software*, Siemens Analytical X-ray Systems, Inc., Madison, WI (1996).

[16] G.M. Sheldrick. *SHELXTL V5.1, Software Reference Manual*, Bruker AXS, Inc., Madison, WI (1997).

[17] Y. Kanda, K.Y. Lee, S. Nakata, S. Asaoka, M. Misono. *Chem. Lett.*, **17**, 139 (1988).

[18] J. Yang, M.J. Janik, D. Ma, A. Zheng, M. Zhang, M. Neurock, R.J. Davis, C. Ye, F. Deng. *J. Am. Chem. Soc.*, **127**, 18274 (2005).

[19] S.K. Kurtz, T.T. Perry. *J. Appl. Phys.*, **39**, 3798 (1968).